

Fine-mapping of DNA damage and repair in specific genomic segments

Herman L. Govan, III, Yadira Valles-Ayoub and Jonathan Braun

Department of Pathology and Jonsson Comprehensive Cancer Center, UCLA School of Medicine, Los Angeles, CA 90024 – 1732, USA

Received April 6, 1990; Revised and Accepted May 21, 1990

ABSTRACT

The susceptibility of various genomic regions to DNA damage and repair is heterogeneous. While this can be related to factors such as primary sequence, physical conformation, and functional status, the exact mechanisms involved remain unclear. To more precisely define the key features of a genomic region targeted for these processes, a useful tool would be a method for fine-mapping gene-specific DNA damage and repair *in vivo*. Here, a polymerase chain reaction-based assay is described for measuring DNA damage and repair in small (< 500 bp) genomic segments of three transcriptionally active but functionally distinct loci (rearranged immunoglobulin heavy chain variable region [Ig VDJ], low-density lipoprotein receptor gene, and *N-ras* proto-oncogene) in human tonsillar B lymphocytes. Analysis of ultraviolet (254 nm)-induced DNA damage revealed single-hit kinetics and a similar level of sensitivity ($D_{50\%} \sim 6000$ joule/m²) in all three regions, indicating that a single photoproduct was sufficient to fully block PCR amplification. A similar time period per unit length was required for repair of this DNA damage (average $t_{1/2}$ per fragment length = 23.5 seconds per bp). DNA damage and repair was also detectable with the base adducting agent, 4-nitroquinoline-1-oxide. However, in this case IgVDJ differed from segments within the other two loci by its relative inaccessibility to alkylation. This assay thus permits high-resolution mapping of DNA damage and repair activity.

INTRODUCTION

DNA damage is a common biologic occurrence against which elaborate enzymatic repair systems have evolved (1, 2). A recent advance in this area has been the development of novel Southern hybridization-based assays which provide a general method for measuring gene-specific DNA damage and repair (3–7). An important contribution of these approaches has been detection of heterogeneous patterns of repair activity within different types of genomic regions (*eg.*, expressed versus non-expressed genes, nuclear matrix attachment sites, origins of replication, and coding versus non-coding strands) and between rodent and primate species. These observations draw attention to the need for fine mapping of these regions, so that the role of distinct sequence

elements and their associated DNA-binding proteins can be correlated with DNA repair accessibility. However, detailed mapping by Southern blot analysis is often constrained due to the lack of suitable restriction enzyme recognition sites. This method is also unsuitable for the study of multi-member gene families, because their inherent polymorphism may result in considerable restriction fragment length diversity, or even (as in the case of Ig VDJ segments polyclonal B lymphocyte populations) the absence of discernable signal.

To overcome this problem, we have designed a new approach based on the polymerase chain reaction (PCR). DNA polymerases typically are unable to synthesize across a damaged nucleotide residue (8,9); in the case of *Taq* polymerase, this has been demonstrated in the context of a PCR-based UV footprinting assay (10). Therefore, we reasoned that by establishing quantitative PCR reaction conditions, the fraction of gene segments bearing one or more damaged nucleotides would be reflected as a proportional reduction in the amount of amplified product. Moreover, DNA repair at the gene segment should be measurable as a restoration in the level of amplified product when cells bearing damaged DNA are cultured for periods of time prior to DNA extraction. Here, we report the development of this assay, and its application to the detection of base lesions and their repair in IgVDJ and other gene segments in human B lymphocytes.

MATERIALS AND METHODS

Cells

Lymphocytes were isolated from surgical tonsillectomy specimens from human palatine tonsils (generously provided by Dr. G. Higgins of the Department of Pathology, Kaiser-Permanente Hospital, Panorama City, CA). Tonsil tissue in complete culture media [RPMI-1640 supplemented with antibiotics, fetal calf serum (20%), sodium pyruvate (1 mM), and β -mercaptoethanol (5×10^{-5} M)] was gently teased apart using sterile, glass pasteur pipettes/forceps. Cells released using this procedure were gently centrifuged ($600 \times g$, 4°C for 10 minutes) through a Ficoll-Hypaque cushion to remove dead cells. Contaminating T lymphocytes were removed from the resulting cells using sheep erythrocyte depletion (11). Flow cytometric analysis for CD20 and CD3 confirmed the identity of the cells as B lymphocytes (>95%). All studies were approved by the Human Subjects

Protection Committees of UCLA and Southern California Kaiser-Permanente Medical Group.

Ultraviolet (UV) treatment of lymphocytes

Genomic DNA containing cyclobutane pyrimidine dimers was prepared by irradiation of B lymphocytes in suspension in ice-cold phosphate-buffered saline (PBS) (4.3 mM Na₂HPO₄, 1.4 mM KH₂PO₄, 137 mM NaCl) in a petri dish on ice (10⁸ cells/mL) at an incident dose rate of 10–20 joule/m²/sec using 254-nm light from a commercial germicidal lamp (8-watt low-pressure mercury vapor source (Sylvania) held in a Gates MR-4 fixture) calibrated with a BLAKRAY® J225 UV meter. Following irradiation, the cells were diluted to approximately 10 mL using complete culture medium (final cell concentration, 10⁵ cells/mL) and either used immediately to prepare genomic DNA or placed in sterile, plastic tissue culture flasks. The flasks of treated cells were incubated at 37°C in 5% CO₂ for 1 to 24 hours prior to permit a period of DNA repair prior to extraction of genomic DNA.

4-NQO treatment of lymphocytes

4-nitroquinoline-1-oxide (4-NQO) was dissolved by gently warming to ≥ 90°C in ethanol. A 10 mg/mL working stock solution was prepared and subsequently serially diluted in duplicate cell suspensions (10⁸ cells/mL) to provide a final treatment concentration of 0.4 μg/mL. Following a standard exposure period (30 minutes at 37°C), the treated cells were washed twice using PBS, diluted in culture medium, and handled as described above to permit different periods of DNA repair followed by extraction of genomic DNA.

Preparation of genomic DNA

Total genomic DNA was prepared as previously described (12). Briefly, samples of 10⁵ to 10⁶ treated/untreated lymphocytes were centrifuged twice (600×g, 4°C for 10 minutes) using 1×PBS. Pelleted cells were resuspended to 10⁷ cells/mL using genomic DNA isolation buffer (10 mM Tris-HCl, pH 8.0; 100 mM NaCl; 25 mM EDTA; 0.5% SDS). The cell suspensions were made 100 μg/mL in proteinase K (BRL) and incubated overnight at 55–60°C. The cleared lysates were extracted twice using phenol and once using chloroform: isoamyl alcohol (24:1 vol:vol). Aqueous layers were separated from organic layers, adjusted to 3.75 M ammonium acetate and precipitated using two volumes of absolute ethanol. Nucleic acids were harvested via centrifugation for 10 minutes in a refrigerated microcentrifuge at 10,000 rpm. Pelleted DNAs were gently resuspended in 10 mM Tris-HCl, pH 8.0, 1 mM EDTA.

Quantitative PCR analysis

Oligonucleotide primers were prepared by Dr. T. Sutherland, MBI preparations facility, UCLA:

- V_H1: 5' dTCTGGGGCTGAGGTGAAGAAG, complementary to a conserved segment on the anti-sense strand within the framework 1 region of human Ig V_H1 genes (13);
- J_HKOR: 5' dACCTGAGGAGACGGTGACCAGGGT, complementary to the most 3' region of the sense strand of consensus human heavy-chain Ig joining(J_H) genes (14);
- LDLrA: 5' dAGTGCCAACCGCCTCACAGG, complemen-

tary to a sense strand segment within exon 14 of the human low-density lipoprotein receptor (LDLr) gene (15);

– LDLrB: 5' dCCTCTCACACCAGTTCACCTC, complementary to a anti-sense strand segment within exon 15 of the LDLr gene (15);

– ras83: 5' dGATTCTTACCGAAAGCAAGTG, 90.5% complementary to an anti-sense strand segment within exon II of the human N-ras proto-oncogene. (16);

– ras84: 5' dATAATAACTACCGTTTATGTG, complementary to a sense sequence within exon III of the human N-ras proto-oncogene (16).

Amplifications were carried out based on the method of Saiki *et al.* (17). In this study, quantitative PCR reaction conditions were required; the key modification required for this purpose is establishing a limiting concentration range for template DNA (18–22). Therefore, the amount of genomic DNA was titrated in pilot experiments to establish a template range in which the amount of template was linearly related to the amount of amplified product. Using tonsil DNA, these primers, and standard reaction conditions (see following), such a range was found at ~20 to 200 ng template DNA per reaction (22). Reactions were performed as follows: 100 ng of pre-denatured (94°C, 2 minutes) genomic DNA templates, 1–2 units of *Taq* DNA polymerase (Perkin-Elmer/Cetus), and 100 picomoles of each primer per reaction (100 microliters, total final volume). Radioactive amplification products were prepared by supplementing individual PCR assay mixture dNTP pools with 0.1 μCi of ³²P-α-dCTP (Amersham) (23). All PCR assay mixtures were subjected to 40 successive cycles consisting of heat denaturation (94°C, 2 minutes), oligonucleotide annealing, and primer extension (72°C, 1.5 minutes). Oligonucleotide primer pairs were used at the following annealing temperatures: V_H1+J_HKOR: 51°C; LDLrA+LDLrB: 49°C; ras83+ras84: 49°C. Reactions were carried out in either an Ericomp® programmable temperature TwinBlock™ or in a Perkin-Elmer DNA Thermal Cycler®. PCR products were fractionated using either 2.5%/1.5% Nu-sieve®/SeaKem® (FMC) agarose gels in 1×TPE buffer (0.08 M Tris-phosphate, 0.008 M EDTA) or 1%/1% Nu-sieve/LE agarose gels in 1×TAE (0.04 M Tris-acetate, 0.002 M EDTA) buffer. Gels were briefly stained in an aqueous solution of 0.1 μM ethidium bromide prior to visualization of amplified DNAs. The sizes of the amplified products were: N-ras, 147 bp; LDLr, 257 bp; IgVDJ, 440 bp. Following electrophoretic fractionation of the amplified products, the agarose gels were dried, covered with plastic wrap and autoradiographed by placing in contact with x-ray film (Kodak X-OMAT™AR) for 4 to 24 hours at –80°C. The autoradiographs were used as templates to excise gel slices. The radioactive gel slices were placed in borosilicate glass counting vials and Cerenkov counts measured using a Beckman LS-7000® scintillation counter. Duplicate samples were typically processed, and reported as arithmetic means; the standard errors were less than 10%.

Spectrophotometric quantitation of 4-NQO adducts

Aliquots of isolated genomic DNAs from 4-NQO-treated lymphocytes were diluted in distilled water, and 500 microliters (total final volume) samples analyzed in a Beckman DU-7® spectrophotometer. The presence of 4-NQO-induced adducts in each sample was determined and is reported as the ratio of the absorbances measured at 354 nm (6) and 260 nm (NQO:DNA).

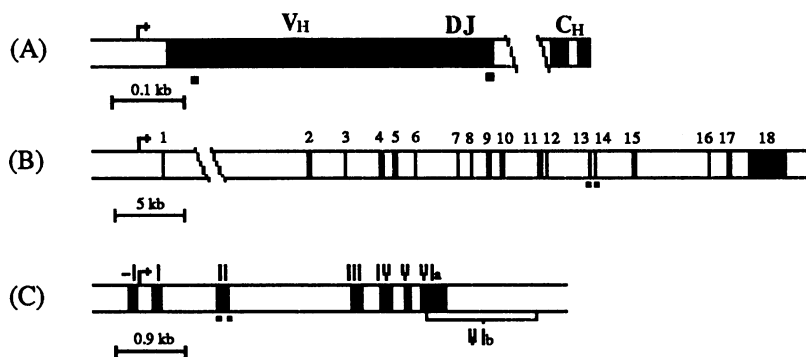


Figure 1. Schematic representation of the genomic organization of (A) IgVDJ, (B) *N-ras*, and (C) LDL receptor (LDLr) loci. Solid segment, exon; open segment, intron or flanking region; hooked arrow, transcriptional start site; ⁿ, amplified region.

Activity of *Taq* DNA polymerase with UV-irradiated template DNA

Microgram quantities of the 147 bp *N-ras* genomic segment were prepared by PCR amplification (as described above, but without radiolabeled nucleotides), agarose gel electrophoresis, phenol/chloroform extraction, and sodium acetate/ethanol precipitation. The segment preparation was dissolved in TE, aliquoted in microtiter wells (500 ng/well), and UV-irradiated to a final dose of 0–24 kJ/m². 50 nanogram samples of the irradiated DNA were then subjected to three PCR cycles using a single [³²P]*ras*83 primer prepared with T4 polynucleotide kinase (Pharmacia, Piscataway, NJ) and [γ -³²P] ATP (ICN, Irvine, CA) (12). Resulting single strand-products were fractionated in a 7M urea/12% polyacrylamide gel, and autoradiographed (without intensifying screen) with x-ray film as described above. The gel also included dideoxy DNA sequencing tracks generated with the 147 bp *N-ras* genomic segment, [³²P]*ras*83 primer, and *Taq* polymerase.

RESULTS

Three genes were selected for study based on their functional diversity and active transcriptional status in human B lymphocytes (24–26). The molecular organization of these genes and the location of the gene segments selected for amplification are shown in Figure 1. The studies were performed on fresh human B cells isolated from surgical tonsillectomy specimens by Ficoll-Hypaque purification of mononuclear cells and sheep erythrocyte depletion of T lymphocytes as described in *Materials and Methods*. In the case of the Ig locus, specific amplification of rearranged IgVDJ segments was achieved using pairs of oligonucleotide primers spanning the recombination site (i.e., 5' V_H and 3' J_H), and the selection of V_H subfamily-specific primers (19, 22, 27,28).

The magnitude of UV dose needed to produce polymerase-blocking damage in genomic DNA was initially determined by irradiating separate B lymphocyte cultures with increasing doses of 254-nm light. Genomic DNA was immediately isolated from the irradiated cells and 100 ng aliquots were amplified in quantitative PCR reactions. As expected, autoradiographic analysis of the gel-fractionated, amplified material demonstrated a dose-dependent loss of radiolabeled product, presumably due to the accumulation of UV photoproducts (Figure 2). These data were recalculated as the fraction of residual damaged (unamplifiable) DNA, and tested for conformity to a first-order

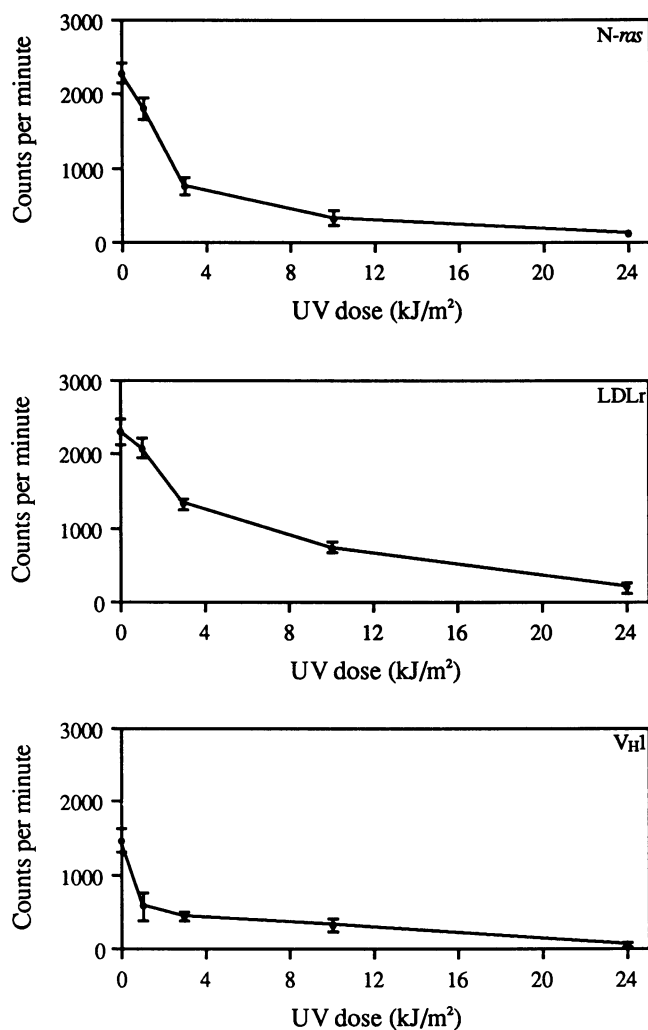


Figure 2. Dose response course for UV-induction of DNA damage. Separate aliquots of 10⁷ tonsillar B lymphocytes were UV-irradiated (254-nm) at 10–20 joule/m²/sec for various times. Genomic DNA was then isolated and amplified by quantitative PCR for IgVDJ (V_H1), LDLr, and *N-ras* gene segments. Values plotted are the calculated means from three experiments (Cerenkov counts expressed as counts per minute [cpm]) obtained from excised gel slices.

dose-dependent model (Figure 3). Regression analysis of the data yielded an excellent fit to this model ($r^2 > 0.9$), and the UV dose required to produce polymerase-blocking lesions in one-

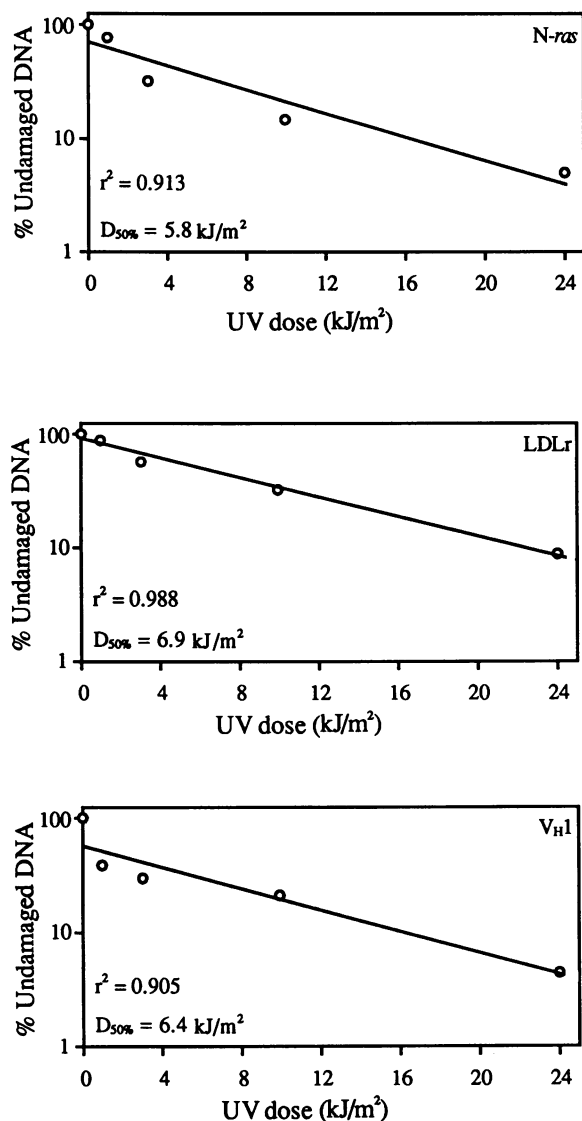


Figure 3. Regression analysis of ultraviolet DNA damage. Values from Figure 2 were recalculated as the fraction of undamaged DNA (F):

$$F = (\text{cpm}_{\text{experimental}}) / (\text{cpm}_{\text{untreated}})$$

and fitted by linear regression to a first-order function, $\log F = md$, where d = dose (in kJ/m²), using CricketGraph software (Cricket Software; Malvern, PA).

half of the susceptible sites ($D_{50\%}$) was calculated from the regression analysis to be 6.4, 6.9 and 5.8 kJ/m² for IgVDJ, LDLr, and N-ras, respectively. These estimates of UV-induced damage closely correspond (within a factor of 2–3) to measurements in kidney fibroblasts using a direct thymine dimer assay (29).

Repair of the ultraviolet-induced DNA damage was then assessed by observing whether reculture of the irradiated cells restored the template activity of the subsequently extracted genomic DNA (Figure 4). In DNA extracted immediately after irradiation (24 kJ/m²), PCR products were reduced 10 to 20-fold compared to DNA from untreated cells. Assuming that the initial data represent zero-class Poisson measurements (11), this level of damage corresponded to 2 to 3 (i.e., $\log_{10}[100]$ or $\log_{10}[1000]$) pyrimidine dimers per gene segment, agreeing well with Figure 2 and values calculated from Williams and Cleaver (3–10 dimers, ref. 29). When the irradiated cells were recultured to allow a period of DNA repair, a progressive and eventually complete restoration of gene segment amplification was observed. These data were recalculated as the fraction of residual damaged (unamplifiable) DNA, and tested by regression analysis for conformity to a first-order kinetic model (Figure 5). An excellent correlation was demonstrated ($r^2 > 0.9$), and the calculated $t_{1/2}$ for repair (3.61 hours for IgVDJ, 1.43 hours for LDLr, 0.852 hours for N-ras) was directly proportional to the gene segment length (23.5 ± 3.0 seconds per bp).

These findings strongly suggested that UV-induced DNA damage and repair were detectable *in vivo* in the range of 0–24 kJ/m². We desired to confirm that these PCR findings were directly related to the unsuitability of UV-irradiated DNA as a template for *Taq* polymerase. Therefore, purified 147 bp N-ras gene segment was irradiated in the same UV dose range, and then used as a template for extension DNA synthesis with the ras83 primer and *Taq* polymerase under PCR reaction conditions (Figure 4). UV irradiation caused a dose-dependent loss of primer extension (observed at spontaneous polymerase stops, *open arrowhead*), presumably due to proximal UV-induced base lesions either blocking primer hybridization or interfering with *Taq* procession. Novel UV-induced bands were also anticipated at adjacent pyrimidine pairs or clusters, but these were typically dim or indistinct in this dose range. However, one such site was readily detectable within a CCT block (position 49 downstream from ras83, *solid arrowhead*). Adjacent pyrimidines can vary orders of magnitude in their UV photoreactivity (10, 30, 31),

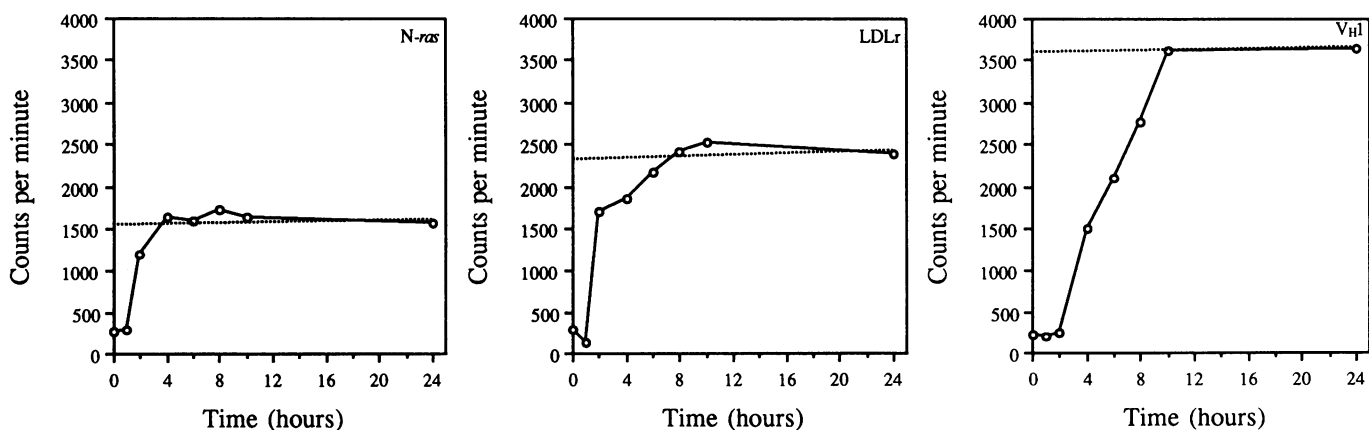


Figure 4. Repair time course of UV-induced DNA damage. Human tonsillar B lymphocytes were UV-irradiated (24 kJ/m²) and cell aliquots were cultured for the indicated time periods to permit an interval of DNA repair. Genomic DNA was then isolated from each cell aliquot, and amplified by quantitative PCR for IgVDJ (V_H1), LDLr, and N-ras gene segments. Values plotted are Cerenkov counts expressed as counts per minute (cpm) obtained from excised gel slices. *Dashed line:* Control PCR quantitation using DNA from untreated cells.

and this may represent a particularly favorable dimer site. This PCR-based method is thus comparable to direct sequencing-based methods previously used for the study of short DNA segments (31).

In a second set of experiments, B cells were treated with 4-NQO, which produces bulky adducts on purine bases (6) presumably capable of interfering with template amplification by blocking *Taq* DNA polymerase procession. Direct spectrophotometric determination of adduct formation in total genomic DNA demonstrated a slow accumulation of base lesions peaking at 4–6 hours, followed by a period of net removal of the 4-NQO-induced adducts (Figure 7). The delayed onset of adduct formation is attributable to several pharmacologic factors, including cellular rate of uptake, microsomal activation (32), and persistence of the reactive species. Hence, the periods of DNA

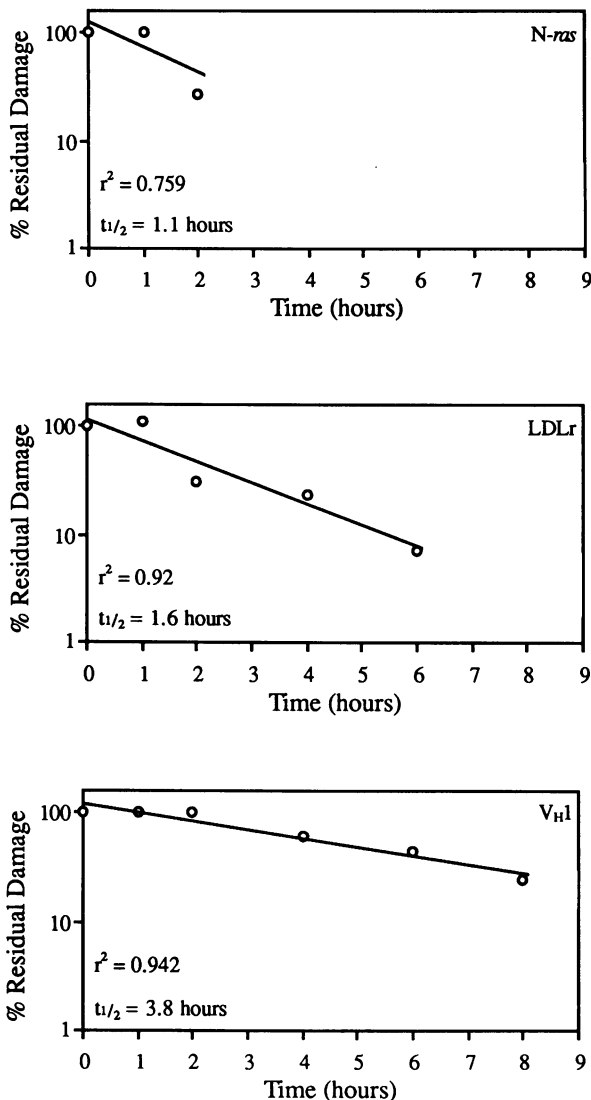


Figure 5. Regression analysis of repair rate for ultraviolet DNA damage. Values from Figure 4 were recalculated as the fraction of residual damaged DNA (*f*):

$$f = 1 - \frac{(\text{cpm}_{\text{experimental}}) - (\text{cpm}_{\text{initial}})}{(\text{cpm}_{\text{control}}) - (\text{cpm}_{\text{initial}})}$$

and fitted via linear regression analysis to a first-order function, $\log f = m t$, where *t* = time (in hours), using CricketGraph software (Cricket Software; Malvern, PA).

damage and repair temporally overlap. However, the loss and restoration of IgVDJ amplification in DNA from treated cells correlated well with the inverse pattern of adduct formation in total genomic DNA (Figures 7 and 8). Surprisingly, the level of LDLr and *N-ras* amplification followed a markedly different time course (compared to that observed for IgVDJ) with an early peak of damage and a rapid restoration of amplifiable DNA, particularly in the case of *N-ras* (Figure 8).

DISCUSSION

We have introduced a PCR-based assay for gene-specific DNA damage and repair, predicated on the capacity of base lesions to interfere with *Taq* polymerase procession. Several observations support the validity of this assay. In the case of UV irradiation, the measured level of initial damage correlated well with published estimates for pyrimidine dimer formation. DNA repair, reflected by a restoration in amplifiable DNA following brief periods of cell culture, was rapid and complete at all three selected gene segments, and proportional to gene segment length. DNA damage and repair induced by 4-NQO was also detectable by this assay, and in the case of IgVDJ, corresponded to the abundance of NQO adducts in bulk DNA determined by

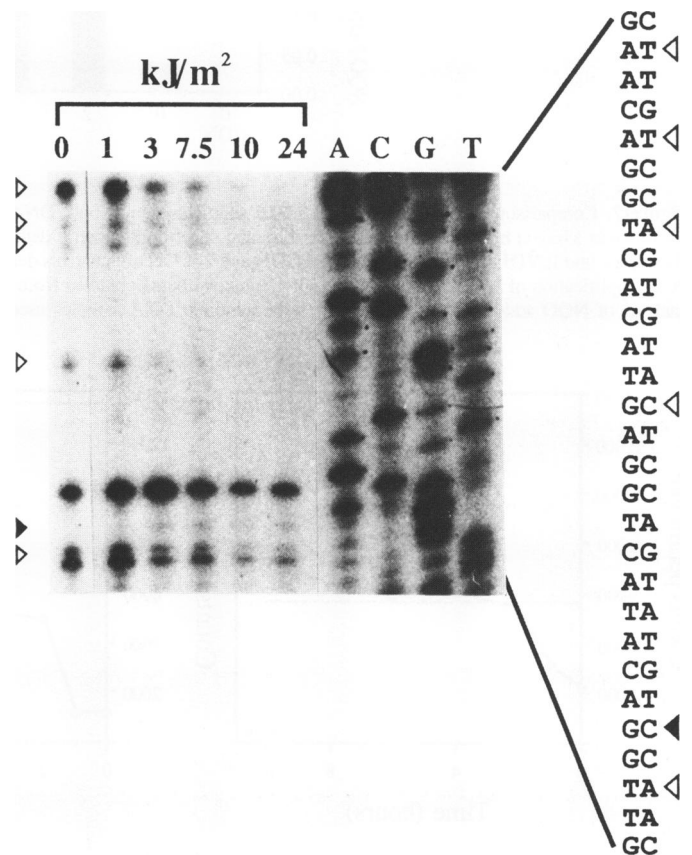


Figure 6. UV-induced DNA damage renders templates unsuitable for *Taq*-mediated DNA synthesis. The 147 bp *N-ras* DNA segment (synthesized by PCR) was UV-irradiated at the indicated doses. DNA (50 ng) from each irradiated sample was then subjected to PCR using a ³²P end-labeled *ras83* oligonucleotide primer, and fractionated on a 12% denaturing polyacrylamide gel. Sequencing tracks with the indicated dideoxy nucleotides are also shown (A, C, G, T). Open arrowheads indicate UV dose-dependent loss of *Taq* procession to the natural stop sites. Filled arrowhead shows a novel, UV-induced stop site at position 49 (downstream from *ras83* primer) occurring within a CCT block.

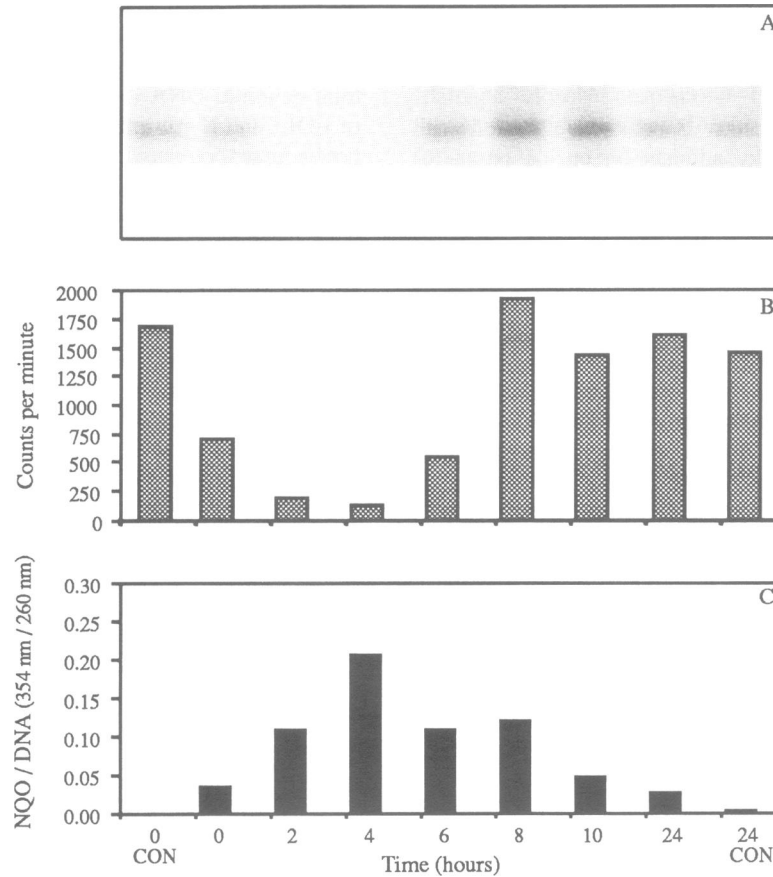


Figure 7. Comparison of 4-NQO repair in IgVDJ segments versus bulk DNA. Genomic DNA obtained from 4-NQO-treated B lymphocytes after indicated time periods was assayed both for IgVDJ amplification and spectrophotometric determination of 4-NQO adducts. Note the consistent inverse correlation between adduct abundance and IgVDJ amplification. Values 0CON and 24CON are controls derived from sham-treated lymphocytes. (A) Autoradiograph depicting quantitative PCR amplification of IgVDJ. (B) Bar graph of Cerenkov counts obtained from excised gel slices corresponding to autoradiographic signals. (C) Spectrophotometric analysis of NQO adducts in aliquots of the same genomic DNA samples used for PCR determinations.

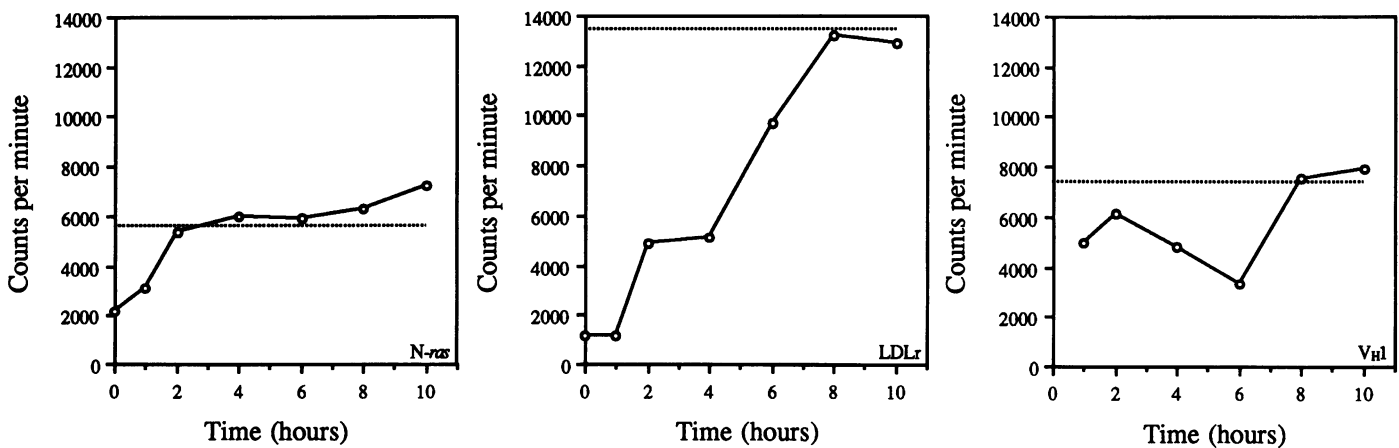


Figure 8. Repair time course of DNA damage induced by 4-NQO. B lymphocytes were treated with 0.4 $\mu\text{g/ml}$ 4-NQO for 30 minutes, then washed and re-cultured for the indicated time periods. Genomic DNA was obtained from 4-NQO-treated lymphocytes and assayed using quantitative PCR amplification as described in Figure 4.

spectrophotometry. From a technical standpoint, it is also notable that PCR analysis under the present conditions (in particular, limiting template DNA) provides a useful quantitative assay for

relative genomic segment abundance (see also 18,19,21,22). The present findings raise certain issues regarding regional patterns of DNA damage and repair. The rate of DNA repair

(average $t_{1/2} = 23.5$ seconds per bp, or 6.5 hours per kb) was consistent among the three tested gene segments, but slow compared to other reported rates of DNA repair rate calculated in this fashion: 4–5 hours for ~20 kb DHFR restriction fragments, or $t_{1/2} \sim 0.2$ hours per kb; $t_{1/2} = 4.5$ hours for total cellular repair synthesis (33). This discordance may be due in part to experimental factors: in the case of DHFR, the accelerated repair rate may be a peculiarity of the highly amplified state of the locus, cell types (epithelioid cell lines versus freshly isolated lymphocytes), and much lower UV dose. A more conceptual possibility is based on the reported segregation of repair synthesis into numerous, simultaneously-active patches spanning 70–100 nucleotides (35). Accordingly, the large DNA segments analyzed in the latter cases undergo disproportionately rapid repair because they encompass multiple repair patches. In contrast, the small segments employed in the present paper are probably spanned by single repair patches, and hence reflect a length-proportionate repair rate.

In a recent study using a Southern blot hybridization DNA repair assay and strand-specific probes, Mellon *et al.* observed rapid and complete repair of the transcribed strand, but deficient repair of the non-coding strand (4). In contrast, UV-damaged DNA segments in the present study were fully repaired at a rapid rate, suggesting that both strands were efficient repair substrates. The difference in outcome may be attributable to technical factors which cause us to overestimate the degree of repair—no prior fractionation of non-replicated DNA was included in the preparation of genomic DNA samples, and the mean UV dose was greater than one dimer per segment length. However, we would like to raise as a second possibility, that the suppression of repair in the non-transcribed strand may occur only within small DNA segments. The apparent rate of DNA repair within a DNA segment is probably limited to that of the slowest contained segment, even if it represents only a very small island within the total DNA segment being analyzed. In the case of Mellon *et al.*, the regions analyzed were much larger (5 to 20 kb) than those examined in the present study (0.1 to 0.5 kb). Accordingly, the segments selected in our study may happen to represent regions which are very efficiently repaired on both strands. At issue then is whether such heterogeneity in non-coding strand repair exists, and if so, the abundance and distribution of such repair-suppressed islands. Using the strategy reported in this study, it should be possible to analyze DNA repair activity occurring within discrete regions to create a comprehensive, contiguous repair map.

With regard to 4-NQO alkylation, it was surprising that whereas IgVDJ damage corresponded to bulk DNA adduct formation, LDLr and N-ras damage occurred in a distinct, accelerated pattern. This relative protection of IgVDJ segments and bulk DNA to chemical alkylation may be due to a distinct chromatin structure or array of DNA-associated proteins which render these regions less accessible to adduct formation. In the case of IgVDJ, this finding may be analogous to the methylation protection observed in some regions of the Ig heavy-chain enhancer (36). From a practical standpoint, this raises the possibility that the present PCR approach may offer a novel analogue to chemical footprinting as a quantitative assay for chromatin structure and the presence of DNA-binding proteins (as suggested in ref. 10).

The present work offers a unique opportunity to observe DNA damage and repair in rearranged Ig variable gene segments of natural B lymphocyte populations. Somatic mutation is involved

in the physiologic diversification of immunoglobulin (Ig) genes at two stages in B lymphocyte (B cell) development. During the pre-B cell stage, combinatorial association of individual Ig gene segments yielding functional light-chain variable genes (VJ_L) and heavy-chain variable genes (VDJ_H) may be accompanied by junctional deletions and N-region insertions (primarily in the latter case) segregated to the coding but not signal joints (37–40). During the early memory B cell stage, the genomic region enveloping the V(D)J segment is subject to a brief but intense period of hypermutation, resulting in the abundant accumulation of nucleotide substitutions/point mutations (26,41,42). The biochemical nature of the mechanisms mediating these processes is largely unknown; however, one appealing component may be selective suppression of certain efficient DNA repair mechanisms at the V(D)J segment, allowing error-prone mechanisms to predominate (26). Using the present approach, it may now be possible to directly test the role of cellular DNA repair mechanisms in B cells isolated at critical points in differentiation when mechanisms of Ig diversification are active; and, to generate a detailed map of the regions within the Ig locus subject to these diversification mechanisms.

ACKNOWLEDGEMENTS

Supported by United States Public Health Service CA12800 and a UCLA AIDS Clinical Research Grant. H.L.G. III is a predoctoral fellow of the Ford Foundation, National Research Council. Y.V.-A. is a postdoctoral fellow of the Fogarty Program in AIDS Research at UCLA. J.B. is a Scholar of the Leukemia Society of America, and a recipient of an RJR-Nabisco Research Scholars Award. We are grateful to Dr. Gerald Higgins and members of the Department of Pathology, Kaiser-Permanente Hospital, Panorama City for tonsil specimens; Lily King for key contributions to the development of the quantitative PCR assay; Drs. Kevin McEntee, Lynn Gordon, and Colin Hill for helpful discussions; and, Carol Appleton for photographic work.

REFERENCES

1. Friedberg, E.C. (1985) DNA Repair. W.H. Freeman, New York.
2. Friedberg, E.C., and Hanawalt, P.C., editors. (1988) Mechanisms and Consequences of DNA Damage Processing. Alan Liss, New York.
3. Mellon, I., Bohr, V.A., Smith, C.A., and Hanawalt, P.C., (1986) Proc. Natl. Acad. Sci. USA **83**: 8878–8882.
4. Mellon, I., Spivak, G., and Hanawalt, P.C. (1987) Cell **51**: 241–249.
5. Ho, L., Bohr, V.A., and Hanawalt, P.C. (1989). Mol. Cell. Biol. **9**: 1594–1603.
6. Thomas, D.C., Morton, A.G., Bohr, V.A., and Sancar, A. (1988) Proc. Natl. Acad. Sci. USA. **85**: 3723–3227.
7. Leadon, S.A., and Snowden, M.M. (1988) Mol. Cell. Biol. **8**: 5331–5338.
8. Moore, P.D., and Strauss, B.S. (1979) Nature **278**:664–666.
9. Chan, G.L., Doetsch, P.W., and Haseltine, W.A. (1985) Biochemistry **24**:5723–5728
10. Axelrod, J.D., and Majors, J. (1989) Nucl. Acid Res. **17**: 171–183.
11. Mishell, B. B., and Shiigi, S.M. (1980) Selected Methods in Cellular Immunology. W.H. Freeman and Company, San Francisco. pp. 205–208.
12. Ausubel, F.M., Brent, R., Kingston, R.E., Moore, D.D., Smith, J.A., Seidman, J.G., and Struhl, K. (1988) Current Protocols in Molecular Biology. John Wiley & Sons, New York. pp. 2.2.1–2.2.3.
13. Berman, J.E., Mellis, S.J., Pollock, R., Smith, C.L., Suh, H., Heinke, B., Kowal, C., Surti, U., Chess, L., Cantor, C.R., Alt, F.W. (1988) EMBO J. **7**:727–738.
14. Crescenzi, M., Seto, M., Herzig, G.P., Weiss, P.D., Griffith, R.C., and Korsmeyer, S.J. (1988) Proc. Natl. Acad. Sci. USA **85**: 4869–4873.
15. Li, H., Gyllenstein, U.B., Cui, X., Saiki, R., Erlich, H.A., and Arnheim, N. (1988) Nature **335**: 414–417.

16. Guerrero, I., Villasante, A., Corces, V., and Pellicier, A. (1985) *Proc. Natl. Acad. Sci. USA* **82**: 7810–7814.
17. Saiki, R.K., Scharf, S., Faloona, F., Mullis, K.B., Horn, G.T., Erlich, H. A., and Arnheim N. (1985) *Science* **230**: 1350–1354.
18. Syvanen, A.C., Bengtstron, M., Tenhunen, J., and Soderlund, H. (1988) *Nucleic Acids Res.***16**: 11327–11338.
19. Schliessel, M.S., and Baltimore, D. (1989) *Cell* **58**:1001–1007.
20. Becker-Andre, M., and Hahlbrock, K. (1989) *Nucleic Acids Res.* **17**:9437–9446.
21. Frye, R.A., Benz, C.C., and Liu, E. (1989) *Oncogene* **4**:1153–1157.
22. Valles-Ayoub, Y., Govan, H.L.III, and Braun, J. (1990) *Blood*, *in press*.
23. Schowalter, D.B., and Sommer, S.S. (1989) *Analytical Biochem.* **177**: 90–94.
24. Levy, N.S., Malipiero, U.V., Lebecque, S.G., and Gearhart, P.J. (1989) *J. Exp. Med.* **160**: 2007–2019.
25. Klinman, D.M., Mushinski, J.F., Homda, M., Ishigatsubo, Y., Mountz, J.D., Raveche, E.S., and Steinberg,A.D. (1986) *J. Exp. Med.* **163**: 1292–1307.
26. Bilheimer, D.W., Ho, Y.K., Brown, M.S., Anderson, R.G.W., and Goldstein, J.L. (1978) *J. Clin. Invest.* **61**:678–696.
27. Chiang, Y.L., Sheng-Dong, R., Brow, M.A., and Larrick, J.W. (1989) *BioTechniques* **7**:360–366.
28. Orlandi, R., Gussow, D.H., Jones, P.T., Winter, G. (1989) *Proc. Natl. Acad. Sci. USA* **86**: 3833–3837.
29. Williams, J.I. and Cleaver, J.E. (1978) *Biophys. J.* **22**: 265–279.
30. Coulondre, C., and Miller, J. H. (1977) *J. Mol. Biol.* **117**:525–567.
31. Gordon, L. K., and Haseltine, W. A. (1982) *Radiation Res* **89**: 99–112.
32. Galiegue-Zouitina, S., Bailleul, B., and Loucheux-LeFebvre, M.H. (1983) *Cancer Res.* **45**: 520–525.
33. Ehmann, U.K., Cook, K. H., and Friedberg, E.C. (1978) *Biophys. J.* **22**:249–264.
34. Keyse, S.M., and Tyrrell, R.M. (1987) *Carcinogenesis* **8**: 1251–1256.
35. Th'ng, J.P.H., and Walker, I.G. (1986) *Mutation Res.* **165**:139–150.
36. Ephrussi, A., Church, G.M., Tonegawa, S., and Gilbert, W. (1985) *Science* **227**: 134–140.
37. Sakano, H., Maki, R., Kurosawa, Y., Roeder, W., and Tonegawa, S. (1980) *Nature (London)* **286**:676–683.
38. Desiderio, S.V., Yancopoulos, G.D., Paskind, M., Thomas, E., Boss, M.A., Landau, N., Alt, F.W., and Baltimore, D. (1984) *Nature* **311**: 752–755.
39. Malynn, B., Blackwell, T., Fulop, G., Rathbun, G., Furley, A., Ferrier, P., Heinke, L., Phillips, R., Yancopoulos, G., and Alt, F. (1988) *Cell* **54**:453–460.
40. Lieber, M.R., Hesse, J.E., Lewis, S., Bosma, G.C., Rosenberg, N., Mizuuchi, K., Bosma, M.J., and Gellert, M. (1988) *Cell* **55**:7–16.
41. Selsing, E., and Storb, U. (1981) *Cell* **25**: 47–58.
42. Gorski, J., Rollini, P., and Mach, B. (1983) *Science.* **220**: 1179–1181.